Catalytic Activity of Highly Dispersed Palladium. II. X-Ray Photoelectron Spectroscopic and Thermal Desorption Studies of the Effects of ZrO_2 Added to α-Alumina-supported Palladium

Bu Yong LEE,* Yasunobu INOUE, and Iwao YASUMORI

Department of Chemistry, Tokyo Institute of Technology, Ookayama, Meguro-ku, Tokyo 152

(Received May 1, 1981)

The effects of ZrO_2 upon the catalytic properties of α-alumina-supported palladium for the hydrogenation of gaseous cyclohexene were studied by means of detailed kinetic analysis, thermal desorption (TD), and X-ray photoelectron spectroscopy (XPS). The catalysts, with ZrO_2 added in amounts ranging from 0.1 to 45 in Zr/Pd ratio, were characterized by CO chemisorption and X-ray diffraction. The addition of ZrO_2 at the Zr/Pd ratio of 0.5 enhanced the turn-over frequency of the hydrogenation by a factor of 7 and changed the hydrogen order of the reaction from 1.0 to 0.75 and the cyclohexene order from 0 to 0.6. The reaction with D_2 exhibited deuterium-distribution patterns similar to those for the reaction on the ZrO_2-supported Pd catalysts. The hydrogenation pathway on the ZrO_2-added catalyst was described by an associative mechanism in which the slow step was a surface reaction between a cyclohexyl radical and a hydrogen atom. In the thermal desorption spectra, the addition of ZrO_2 caused a broadening of the adsorbed hydrogen peak as well as a shift of the dissolved hydrogen peak toward a lower temperature. The desorption of cyclohexene from Pd/α-Al_2O_3 catalysts underwent a disproportionation to produce benzene around 318 K and cyclohexane at 368 K, whereas the latter peak shifted by 70 K to the lower-temperature side upon the addition of ZrO_2. The XPS study showed that the presence of ZrO_2 provided Pd metal atoms in a negatively-charged state. The support effect was discussed on the basis of the interaction between Pd metal atoms and ZrO_2 oxide.

In recent research in heterogeneous catalysis by supported-metal catalysts, it has been recognized that the catalytic and adsorptive properties of metals loaded depend not only on the characteristics of their geometrical structures, but also on the nature of the underlying supports.[1-5] In the first paper of this series,[6] we have reported that the turn-over frequency of the cyclohexene hydrogenation is larger by one order of magnitude for the ZrO_2-supported Pd catalysts than for the α-alumina-supported Pd and Pd black catalysts. The kinetic behavior of the hydrogenation is also different, and it was proposed that there existed a considerable interaction between the dispersed Pd and ZrO_2 surfaces. For a better understanding of this phenomenon, quantitative information on the interaction between the metal and oxide is needed, and thus it is of interest to employ catalysts in which Pd and ZrO_2 were loaded in different ratios on an inert carrier of α-alumina.

The present study aims at comparing the effect of the ZrO_2 codispersed with Pd to the effects of the ZrO_2 support and at revealing how the catalytic properties vary as a function of the atomic ratio of Zr/Pd. Mechanistic analysis based on the detailed kinetics using D_2 as a tracer was applied to the hydrogenation of gaseous cyclohexene over catalysts with different Zr/Pd ratios. Further, the thermal desorption study was undertaken in order to examine the influence of ZrO_2 upon the adsorbed states of hydrogen and cyclohexene.

In an effort to reveal the change in electronic structures which might be induced through the metal-oxide interaction, X-ray photoelectron spectroscopy (XPS) was employed. The controllable atomic ratio of Zr/Pd in the present system makes this XPS analysis more effective than the previous system of Pd supported on ZrO_2, in which the tail of a large Zr 3d peak interfered with an accurate determination of the Pd 3d levels. The geometric structure of Pd metal in the presence of ZrO_2 was characterized by X-ray diffraction and CO chemisorption methods.

Experimental

The procedure of preparing the catalysts, α-alumina-supported Pd and ZrO_2, and the chemical reagents used were the same as those employed previously[6] except for the use of mixed solutions of palladium and zirconyl nitrates. The concentration of palladium was adjusted to maintain a 2.1 wt% of α-alumina for each of the catalysts, while the atomic ratio of Zr/Pd was increased from 0.1 to 45. Prior to the kinetic run, the catalysts were treated with 20 Torr of oxygen (1 Torr=133.3 Pa) at 523 K, reduced with 20 Torr of hydrogen, and then evacuated at the same temperature. The kinetic behavior of the reaction was examined in the temperature range of 283—323 K, using reactants in the pressure range of 10—40 Torr. The apparatus, procedure, and reactant used have been described elsewhere.[6] The crystallite size and the percentage exposed of the dispersed catalysts were determined by means of the CO chemisorption and X-ray diffraction in manners similar to those employed in the previous study.[6]

The X-ray photoelectron spectra were recorded at room temperature on a Hewlett-Packard 5950A ESCA spectrometer with monochromatized Al $K\alpha$ excitation. Each catalyst sample was pressed in the form of pellets, mounted on a recessed quartz plate, and transferred into the XPS preparation chamber, where it was subjected to "*in situ*" treatment similar to the activation used in the kinetic study except for relatively lower pressures of oxygen and hydrogen (≈5 Torr). The background pressure during photoemission measurement was below 3×10^{-9} Torr. The charging shift was compensated for, or at least minimized, by showering low-energy electron by the use of a flood gun. The binding energies of Al $2s_{1/2}$= 119.1 eV and C 1s=284.8 eV were taken as reference.

The thermal desorption spectra were recorded by using a high-vacuum apparatus pumped at such a high speed that the rate of desorption was proportional to the partial pressure

of the desorbing species.[7] This apparatus was equipped with an ionization gauge to monitor the change in the total pressure, and with a quadrupole mass spectrometer, Mitsubishi MF-T_2M, for the analysis of the desorbed molecules. After being subjected to the pretreatments, the catalyst samples were exposed to different pressures of hydrogen or cyclohexene at various temperatures. The temperature of the catalysts was raised at a rate of 13 K min^{-1} by the use of an outside electric furnace, and was monitored with a Pt–Pt/13%Rh thermocouple which was directly brought into contact with the samples.

Results

Figure 1 shows the variation in the catalytic activity, V_g, as a function of the Zr/Pd ratio. The initial activity, 0.88×10^{21} molecule min^{-1}g-Pd^{-1}, for the 2.1 wt% Pd/α-Al_2O_3 catalyst increased markedly with the addition of ZrO_2 up to a Zr/Pd ratio of 0.5, slowed to a gradual increase, and then reached a stationary value, 4.3×10^{22}, at a ratio of Zr/Pd=45. This activity is in substantial agreement with that for the 2.1 wt% Pd/ZrO_2 catalyst. No catalytic hydrogenation proceeded on the alumina and ZrO_2 under the same conditions. The variations in the pressure and temperature dependence of the hydrogenation rate were systematically examined for the catalysts with different Zr/Pd ratios; the kinetic parameters thus obtained are summarized in Table 1. By the addition of ZrO_2 at a Zr/Pd ratio of 0.5, the reaction order with respect to the hydrogen pressure, P_h, decreased from 1.0 to 0.75, whereas the order with respect to the cyclohexene pressure, P_e, increased from 0 to 0.60. Above this ratio, no significant change was observed, and it should be noted that the values obtained were almost the same as those for the ZrO_2-supported Pd catalysts.[6] There was a similar trend in the variation in the activation energy, E_a, with the addition of the ZrO_2 component.

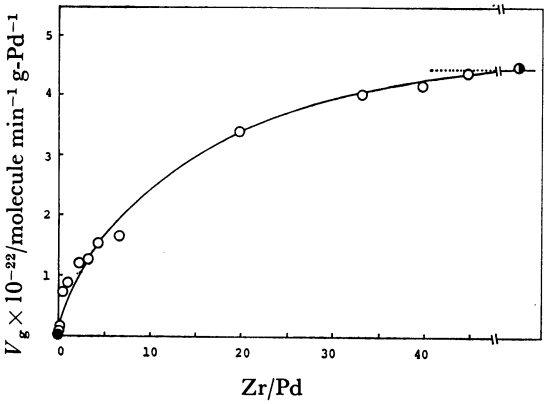

Fig. 1. Variation in catalytic activity, V_g, with Zr/Pd ratio.
P_h=40 Torr, P_e=40 Torr, reaction temperature: 301 K.
●: 2.1 wt% Pd/α-Al_2O_3, ○: ZrO_2-added 2.1 wt% Pd/α-Al_2O_3, ◑: 2.1 wt% Pd/ZrO_2.

Table 1 also shows the results of the characterization of ZrO_2-added Pd catalysts by the CO chemisorption and X-ray line broadening methods, together with the turn-over frequency of the reaction rate, N_t. The percentage exposed, D_{CO}, gradually rose with the increase in the amount of ZrO_2, *e.g.*, by a factor of 1.4 at Zr/Pd=0.5 and of 2.3 at Zr/Pd=2.5, whereas a marked rise in N_t's occurred around the ratio of Zr/Pd=0.3—0.5. Both values converged with those for the 2.1 wt% Pd/ZrO_2 catalyst at Zr/Pd ratios larger than 45.

Table 2 shows the deuterium distributions in the reaction of cyclohexene with D_2 or with an equimolar mixture of H_2+D_2 at 301 K over a catalyst with a Zr/Pd ratio of 0.5. In the case of the former reaction, the cyclohexane product exhibited wide deuterium distributions, ranging from D_0 to D_5, whereas there

Table 1. Characterization of ZrO_2-added Pd/α-Al_2O_3 catalysts and kinetic parameters of cyclohexene hydrogenation

Pd wt%	Ratio of Zr/Pd	V_g[a] molecule / min g-Pd	CO[b] molecule / g-Pd	D_{CO}/%[c]	D_X/%[d]	N_t / s^{-1}	Reaction order[e] m	n	Activation energy[f] E_a / kJ mol^{-1}
2.1	0.0	0.88×10^{21}	1.30×10^{20}	2.2	2.5	0.10	1.00	0.10	38.5
	0.1	2.23	1.37	2.4	1.5	0.27	0.90	0.20	36.7
	0.3	2.79	1.49	2.6	2.1	0.32	0.78	0.33	42.3
	0.5	7.02	1.69	3.0	—	0.69	0.75	0.60	46.3
	1.0	8.61	2.09	3.7	2.8	0.70	0.75	0.63	46.1
	2.5	12.0	2.83	5.0	—	0.71	0.78	0.60	48.1
	3.3	12.3	—	—	—	—	0.76	0.60	47.6
	4.3	15.1	3.49	6.2	—	0.72	0.72	0.60	51.5
	6.5	16.3	—	—	—	—	0.70	0.60	46.1
	20.0	34.2	—	—	—	—	0.77	0.60	51.5
	34.0	40.0	5.25	9.3	—	1.06	0.70	0.60	50.3
	40.0	41.2	—	—	—	—	0.76	0.66	53.3
	45.0	43.3	5.37	9.6	10.1	1.33	0.72	0.67	49.4
2.1 wt%Pd/ZrO_2[g]		44.5	5.71	10.1	9.7	1.35	0.70	0.60	46.1

a) P_h: 40 Torr, P_e: 40 Torr; Reaction temperature: 301 K. b) Saturated adsorption at 301 K. c) Percentage exposed(%) evaluated on the assumption of one CO admolecule on each Pd atom. d) Percentage exposed from X-ray line broadening. e) $V=k\,P_h^m\cdot P_e^n$. f) Temperature range: 283—323 K, ±1.4 kJ mol^{-1}. g) Ref. 6.

also existed exchanged cyclohexene ranging up to D_4. Considerable amounts of HD and H_2 were produced in the gas phase, but the value of K, defined as P_{HD}^2/P_hP_D, remained at 1.3—1.4. The latter reaction with a mixture of H_2 and D_2 gave rise to K=1.4—2.5. These values apparently deviated from that for equilibrium at this reaction temperature, indicating that no equilibrium among H_2, HD, and D_2 in the gas phase was established. It should be noted that the deuterium distributions noted here resembled those obtained for the ZrO_2-supported Pd catalyst rather than those of the α-alumina-supported one.[6] From the above-mentioned variations in N_t, kinetic parameters, and deuterium distribution patterns, one can see that the addition of Zr atoms (as ZrO_2), when its concentration attained about a half of that of Pd atoms, caused an almost complete change in the catalytic properties of the Pd metal.

Table 2. Deuterium distribution in the reaction of cyclohexene with deuterium

Catalyst		2.1 wt%Pd+ZrO_2/α-Al_2O_3 (Zr/Pd=0.5)				
		$D_2+C_6H_{10}$[a]			$D_2+H_2+C_6H_{10}$[b]	
Conversion	(%)	7	10	17	7	17
Cyclohexane	D_0	13	21	17	39	35
	D_1	27	29	32	42	45
	D_2	25	19	25	14	17
	D_3	15	13	13	3	3
	D_4	12	11	9	2	0
	D_5	8	7	4	0	0
	D_6—D_{12}	0	0	0	0	0
Cyclohexene	D_0	87	82	83	93	81
	D_1	6	8	3	3	11
	D_2	2	5	3	2	4
	D_3	2	5	3	2	3
	D_4	2	0	3	0	1
	D_5	1	0	3	0	0
	D_6	0	0	2	0	0
	D_7—D_{10}	0	0	0	0	0
H_2		2	3	4	31	29
HD		15	18	20	37	44
D_2		83	79	76	32	27

Reaction temperature: 301 K; a) $P_D=P_e$=40 Torr, b) $P_h=P_D$=20 Torr, P_e=40 Torr.

Figure 2 shows the X-ray photoelectron spectra in the Pd 3d region. Palladium supported on α-alumina gave the peaks due to Pd $3d_{5/2}$ and $3d_{3/2}$ levels at 335.2 and 340.6 eV respectively. As for the ZrO_2-added catalysts, these peaks shifted to 335.0 and 340.5 eV at Zr/Pd=0.5, and to 334.8 and 340.2 eV at Zr/Pd=2.5, whereas little change was observed with the Zr 3d level. Table 3 lists the binding-energy values.

Figure 3 illustrates the thermal desorption spectra of hydrogen. The desorption from α-alumina-supported Pd catalysts provided three peaks, at α(273 K), β_1(363—383 K), and β_2(460 K). The initial adsorption gave rise to the β_2-peak, and further adsorption developed the β_1-peak. With an increase in the amount of hydrogen

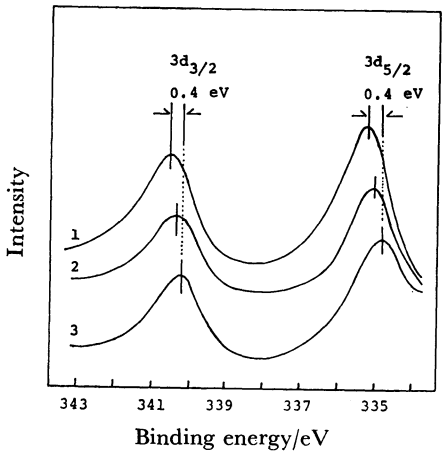

Fig. 2. X-Ray photoelectron spectra in Pd 3d region. 1: 2.1 wt% Pd/α-Al_2O_3, 2: ZrO_2-added 2.1 wt% Pd/α-Al_2O_3(Zr/Pd=0.5), 3: ZrO_2-added 2.1 wt% Pd/α-Al_2O_3(Zr/Pd=2.5).

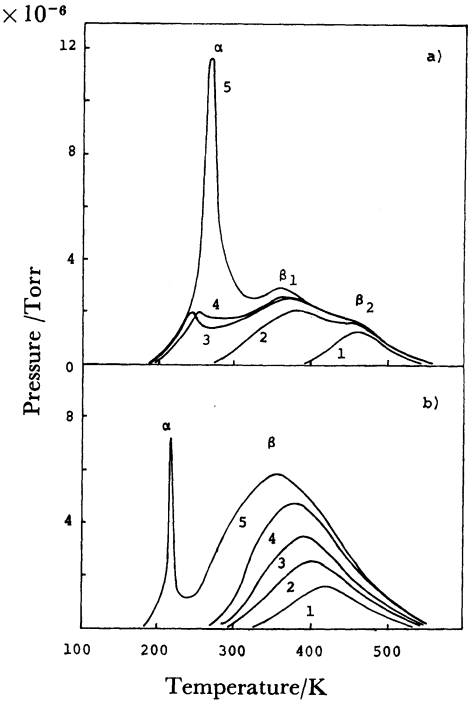

Fig. 3. Thermal desorption spectra of hydrogen.
a) 2.1 wt% Pd/α-Al_2O_3 catalyst exposed to hydrogen at 298 K and cooled to 78 K.
Pressure of hydrogen;
1), 2): below 1×10^{-2}, 3): 3.5×10^{-2}, 4): 7×10^{-2}, and 5): 1.8×10^{-1} Torr.
b) ZrO_2-added 2.1 wt% Pd/α-Al_2O_3 catalyst (Zr/Pd=0.5) under the same conditions as a).
1), 3): below 1×10^{-2}, 4): $\approx1\times10^{-2}$, and 5): 7×10^{-2} Torr.

adsorbed, the β_1-peak shifted to the lower-temperature side by 20 K. After the saturation of the β peaks, the very sharp α-peak began to appear and thereafter grew. In the case of the ZrO_2-added Pd catalyst (Zr/Pd=0.5), the desorption spectra of hydrogen resulted in a broad β peak at 363—413 K, the peak maximum of which shifted to the lower-temperature side with the amount

Table 3. Binding energies of Pd 3d and Zr 3d peaks

Catalysts	Pd		Zr	
	$3d_{5/2}$	$3d_{3/2}$	$3d_{5/2}$	$3d_{3/2}$
$Pd/\alpha\text{-}Al_2O_3$	335.2 eV	340.6 eV	—	—
$Pd+ZrO_2/\alpha\text{-}Al_2O_3$ (1 : 0.5)	335.0	340.5	182.0	184.3
$Pd+ZrO_2/\alpha\text{-}Al_2O_3$ (1 : 2.5)	334.8	340.2	181.9	184.3

Accuracy of the values: ±0.15 eV.

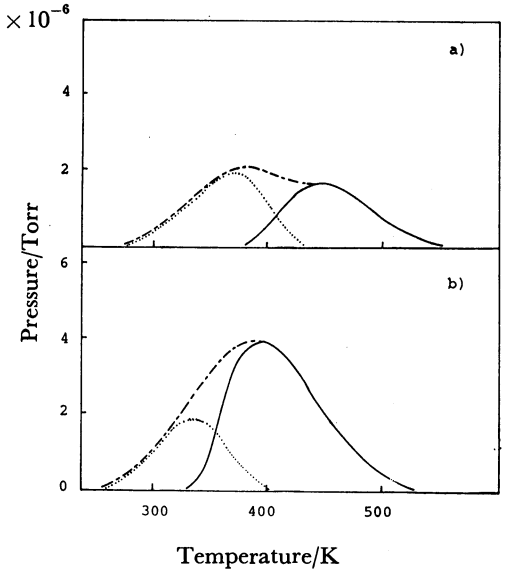

Fig. 4. Thermal desorption spectra of hydrogen contacted with cyclohexene at 195 K. a): 2.1 wt% $Pd/\alpha\text{-}Al_2O_3$, b): ZrO_2-added 2.1 wt% $Pd/\alpha\text{-}Al_2O_3$ (Zr/Pd= 0.5). Dashed line (—·—·): before the contact with cyclohexene, Solid line (——): after the contact, dotted line (····): removed hydrogen by reaction.
In these experiment, desorbing hydrocarbon species were trapped off before entering the mass spectrometer.

of hydrogen adsorbed, whereas the narrower α-peak appeared at 223 K. The TD spectra of hydrogen from the ZrO_2-supported Pd surface were analogous to those for the ZrO_2-added Pd catalyst, except for the appearance of the α-peak at 190 K. Only a small peak of hydrogen was observed around 220 K from α-alumina-supported ZrO_2 without Pd metals.

In order to examine the reactivity of the adsorbed hydrogen, the surface with β-hydrogen was exposed to cyclohexene; as is shown in Fig. 4, the desorption spectra of hydrogen from the $Pd/\alpha\text{-}Al_2O_3$ catalyst resulted in the near disappearance of the β_1-peak, without any significant change in the β_2-peak, whereas those from the ZrO_2-added catalysts lacked the portion on the lower-temperature side of the peak.

The desorption spectra of cyclohexene from the $Pd/\alpha\text{-}Al_2O_3$ surface provided a peak of benzene around 318 K, together with a peak of cyclohexane at 368 K (Fig. 5). In the case of the ZrO_2-added catalyst (Zr/Pd= 0.5), the benzene peak appeared at almost the same temperature, 313 K, while the cyclohexane peak shifted to a temperature lower by 70 K. No peak due to

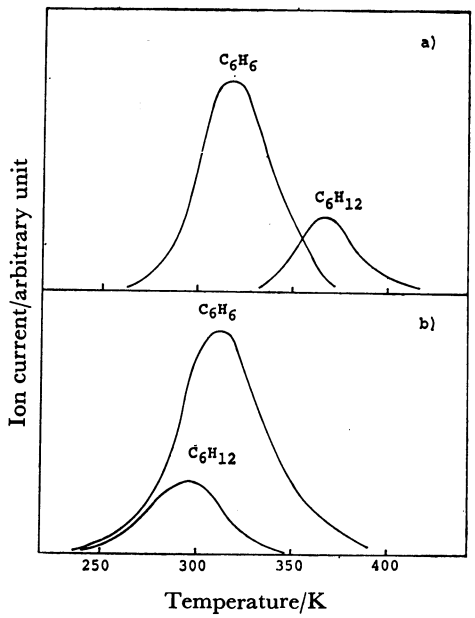

Fig. 5. Thermal desorption spectra of preadsorbed cyclohexene.
a): 2.1 wt% $Pd/\alpha\text{-}Al_2O_3$, b): ZrO_2-added 2.1 wt% $Pd/\alpha\text{-}Al_2O_3$ catalyst (Zr/Pd=0.5). Adsorption temperature: 195 K.

cyclohexene was observed in either catalyst. When hydrogen was preadsorbed, followed by the adsorption of cyclohexene, the resulting desorption spectra exhibited only a cyclohexane peak at 320 K for $Pd/\alpha\text{-}Al_2O_3$ and one at 308 K for the ZrO_2-added catalysts.

Discussion

The present study showed remarkable effects of ZrO_2 upon the catalytic activity of Pd dispersed on α-alumina, and also revealed that the characteristic modification is achieved by a concentration of Zr at 0.5 as the Zr/Pd ratio, since the N_t value was increased significantly; also, the kinetic parameters became almost the same as those for the hydrogenation over Pd/ZrO_2 catalysts. The deuterium distributions also exhibited a characteristic pattern similar to those for ZrO_2-supported Pd catalysts, *i.e.*, a wide deuterium exchange in cyclohexane, but less exchange in cyclohexene, as well as a composition of gaseous hydrogen isotopes far from equilibrium. Therefore, we are able to describe the ZrO_2-affected catalytic hydrogenation by the associative mechanism which was employed in the same reaction on the ZrO_2-supported catalysts:[6]

$$H_2(g) \underset{k_{-1}}{\overset{k_1}{\rightleftharpoons}} 2H(a), \quad (1)$$

$$C_6H_{10}(g) \underset{k_{-2}}{\overset{k_2}{\rightleftharpoons}} C_6H_{10}(a), \quad (2)$$

$$H(a) + C_6H_{10}(a) \underset{k_{-3}}{\overset{k_3}{\rightleftharpoons}} C_6H_{101}(a), \quad (3)$$

$$H(a) + C_6H_{11}(a) \xrightarrow[k_4]{} C_6H_{12}(g), \quad (4)$$

where k_i and k_{-i} denote, respectively, the rate constants of the forward and reverse reactions at the ith step. The formation of highly-exchanged cyclohexanes allows us

to assume that Step 3 is in pseudo-equilibrium. In addition to this assumption, the employment of the steady-state approximation on the concentrations of hydrogen atom, cyclohexene, and the cyclohexyl intermediate leads to the following rate equation:[6]

$$V_g = \frac{2k_1k_4K_2K_3P_hP_e}{[(1+K_2P_e)\sqrt{2k_{-1}+k_4K_2K_3P_e}+(1+K_2K_3P_e)\sqrt{2k_1P_h}]^2}, \quad (5)$$

where $K_i=k_i/k_{-i}$.

Equation 5 is transformed into:

$$\sqrt{\frac{P_h}{V_g}} = \sqrt{\frac{1}{2k_1k_4K_2K_3P_e}}[\sqrt{2k_1P_h}(1+K_2K_3P_e) + (1+K_2P_e)\times\sqrt{2k_{-1}+k_4K_2K_3P_e}], \quad (6)$$

or;

$$\sqrt{\frac{P_e}{V_g}} = \sqrt{\frac{1}{k_4K_1K_2K_3P_h}}[1+\sqrt{K_1P_h} + (1+K_3\sqrt{K_1P_h}+\frac{k_4K_3}{4k_{-1}})K_2P_e], \quad (7)$$

in an approximate form. Figure 6 shows the plots of the $\sqrt{P_e/V_g}$ term *vs.* P_e, and of the $\sqrt{P_h/V_g}$ term *vs.* $\sqrt{P_h}$, for the catalysts with Zr/Pd=0.5 and 1.0 respectively. The good linear relationships verify the validity of the equation, and hence the mechanism proposed.

By analogy with the previous results on the thermal desorption of hydrogen from Pd powder,[7] Pd wire,[8] and Pd/activated carbon,[9] the β_1 and β_2 peaks from the α-alumina-supported Pd catalysts were associated with the adsorbed hydrogen, whereas the α-peak was assigned to the dissolved hydrogen. Judging from the reactivity with cyclohexene, one can reasonably consider that the β_1-hydrogen species is responsible for the hydrogenation. The shift of this peak toward the lower-temperature side with the amount of hydrogen is indicative of a second-order desorption, and hence of the dissociated state of the hydrogen. This supports the aforementioned reaction mechanism.[6] As to the reactivity and dissociated state, similar situations hold for the β-hydrogen on the ZrO_2-added catalyst. Although the separation between β_1 and β_2 peaks is difficult in this case, it is not unreasonable to assume, by taking the reactivity with cyclohexene into account, that the hydrogen located on the lower-temperature side of the β peak is associated with the β_1-state, as is shown by the dotted line in Fig. 4, and that the remaining peak corresponds to the β_2-state. In this classification, there is a tendency for the β_1 and β_2 hydrogens on the ZrO_2-added catalysts to be desorbed at slightly lower temperatures than those on α-alumina-supported Pd catalysts. An other feature of the ZrO_2 effect was the shift of the α peak due to the dissolved hydrogen to a lower temperature. As is shown in Table 4, the temperature of each peak maximum was lowered with an increase in the Zr/Pd ratio. These results suggest that the dissolved hydrogen became unstable with the addition of ZrO_2, in accordance with a weakening of the adsorption bond of hydrogen. Such unstability is partly ascribable to the increase in D_{CO}, *i.e.*, the crystallite-size effect, but the main reason appears to be the changes in the electronic states of dispersed Pd metals.

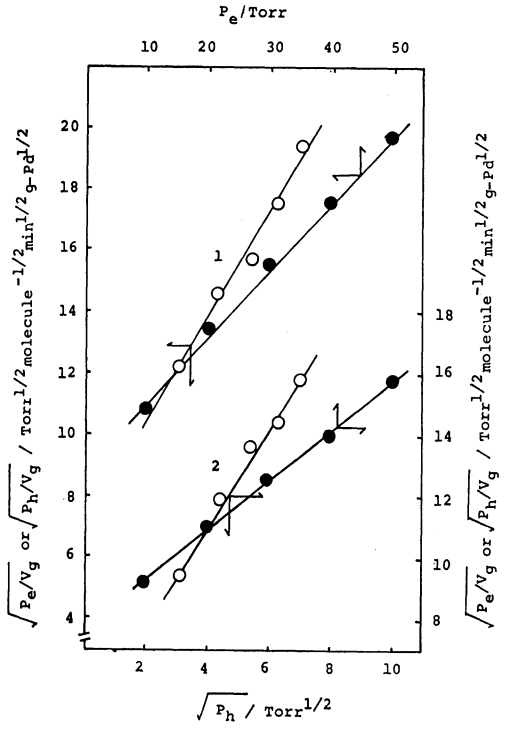

Fig. 6. Rate-partial pressure relationships for cyclohexene hydrogenation on ZrO_2-added 2.1 wt% Pd/α-Al_2O_3 catalysts.
○: $\sqrt{P_h/V_g}$ *vs.* $\sqrt{P_h}$, ●: $\sqrt{P_e/V_g}$ *vs.* P_e.
1): Zr/Pd=0.5, 2): Zr/Pd=2.5.

Table 4. Variation in the peak temperature of α-hydrogen with the Zr/Pd ratio

	2.1 wt% Pd+ZrO_2/α-Al_2O_3					2.1 wt% Pd/ZrO_2
Zr/Pd ratio	0	0.1	0.3	0.5	2.5	
Peak temperature/K	273	253	238	223	190	190

The present XPS study has revealed that the Pd 3d line shifts to a lower binding energy upon the addition of ZrO_2. Provided the contribution of a relaxation effect to the photoemission process is not significantly changed by the presence of the ZrO_2 component, it follows that this shift reflects an increased electron density around surface Pd metal atoms as a consequence of electron transfer from the oxide to Pd metal atoms. According to the DV Xα-calculation of the electronic state for H–Pd_6 and H–Ni_6 clusters,[10] a hydrogen atom on the Pd cluster is slightly negative, in contrast to largely-negative hydrogen on the Ni cluster, and the formation of a stable hydride phase in the Pd–H system is attributable to covalency in bonding between hydrogen and Pd metal atoms. Therefore, it can reasonably be concluded that the transfer of an electron to the Pd metal observed in the present system makes the adsorbed and dissolved hydrogen unstable.

A possible mechanism of benzene and cyclohexane formation during the thermal desorption of cyclohexene is:

$$C_6H_{10}(a) \longrightarrow C_6H_6 + 4H(a), \quad (8)$$

$$C_6H_{10}(a) + 2H(a) \longrightarrow C_6H_{12}, \quad (9)$$

where Step 9 is regarded as being a combination of Steps 3 and 4. The low-temperature shift of cyclohexane, together with the TD result that the cyclohexene adsorbed on the hydrogen-covered surface was desorbed as cyclohexane at a lower temperature in the presence of ZrO_2, suggests that the total energy level of the adsorbed hydrocarbon species including the cyclohexene and/or the cyclohexyl radical becomes higher in the case of the ZrO_2-added Pd catalyst surface. This view is in line with the fact that the apparent activation energy with reference to the energy level of gaseous reactants became higher for the reaction on the ZrO_2-added Pd catalyst than on the Pd/α-Al_2O_3 catalyst. Thus, it may be concluded that the variations in the reaction orders with ZrO_2 addition are mainly to be contributed to the much weakened adsorption of hydrocarbon species compared to that of hydrogen.

The support effects were also observed for TiO_2, the oxide of Group IV_a metals; nickel deposited on this oxide exhibited a stable and high catalytic activity for the methanation reaction of CO.[11] A recent systematic study using XPS, UPS, LEED, and AES[12] revealed that the nickel atoms at the Ni/TiO_2(110) interface are negatively charged as a result of electron transfer through Ni-O^{2-} interaction, which is responsible for the enhanced backdonation of electrons to the $2\pi^*$ orbital of the adsorbed CO molecule, thereby facilitating the dissociation of CO. The negatively-charged state of platinum was also observed to exist on the $SrTiO_3$(100) surface.[13] The SCF Xα-scattered wave calculation for a Pt atom on the $(TiO_6)^{8-}$ cluster[14] showed that the ability of the Pt atom to chemisorb hydrogen was lost when there was a strong interaction between Pt and Ti atoms, whereas the importance of metal-oxygen interaction and the role of the resulting electronic structure in breaking the hydrogen bond were suggested in the Ru/SiO_2 system.[15]

The present TD spectra of hydrogen showed that the chemisorption of hydrogen was not severely suppressed in the presence of ZrO_2. In our IR study of CO adsorbed on silica-supported Pd surfaces, the absorption bands characteristic of the C–O stretching vibration shifted to a frequency lower by 65 cm^{-1} when ZrO_2 was added at the Zr/Pd ratio of 0.5;[16] this shift is evidently ascribable to the enhanced backdonation to the $2\pi^*$ orbital of CO, which was similar to that observed in the above-mentioned Ni–TiO_2 system. From these findings, therefore, it seems reasonable at present to assume that the interfacial interaction between Pd and ZrO_2 occurs through the Pd–O bond, although we need more essential understanding from the theoretical point of view.

The present ZrO_2-added Pd catalysts allow us to consider two structural models. One is that Pd metal and ZrO_2 oxide particles grow almost independently on the alumina surface and can interact each other through the particle-to-particle interface; this requires a long-range interaction for ZrO_2 to exert its effect. Another model is that the Pd metal is mainly deposited on ZrO_2 oxide over α-Al_2O_3. The latter model is more plausible, since the preferential interaction between Pd and ZrO_2 components can be expected, as is revealed by XPS, and since the catalytic properties of the ZrO_2-added Pd catalysts were substantially the same as those of the ZrO_2-supported Pd catalysts. Furthermore, it seems more reasonable to consider that Pd-metal clusters grow on ZrO_2 with a specific structure so as to increase the interfacial boundary-area with the ZrO_2 component than to assume the long-range interaction of the former model.

In order to verify the validity of these models, we have to await precise analysis, *e.g.*, using the EXAFS technique,[17] which will be able to provide information on the composition and microscopic local structure around each of the atoms in these solid mixtures.

References

1) G. M. Schwab, *Adv. Catal.*, **27**, 1 (1976).
2) G. J. Den Otter and F. M. Dautzenberg, *J. Catal.*, **53**, 116 (1978).
3) S. J. Tauster, S. C. Fung, and R. L. Garten, *J. Am. Chem. Soc.*, **100**, 170 (1978).
4) M. A. Vannice and R. L. Garten, *J. Catal.*, **56**, 236 (1979).
5) D. J. C. Yates, L. L. Murrell, and E. B. Prestridge, *J. Catal.*, **57**, 41 (1979).
6) B. Y. Lee, Y. Inoue, and I. Yasumori, *Bull. Chem. Soc. Jpn.*, **54**, 13 (1981).
7) Y. Inoue, I. Kojima, S. Moriki, and I. Yasumori, *Proc. 6th Int. Congr. Catal.*, **1**, 139 (1976).
8) A. W. Aldag and L. D. Schmidt, *J. Catal.*, **22**, 260 (1971).
9) J. A. Konvalinka and J. J. F. Scholten, *J. Catal.*, **48**, 374 (1977).
10) H. Adachi, S. Imoto, T. Tanabe, and M. Tsukada, *J. Phys. Soc. Jpn.*, **44**, 1039 (1978); T. Tanabe, H. Adachi, and S. Imoto, *Jpn. J. Appl. Phys.*, **17**, 49 (1978).
11) M. A. Vannice, *J. Catal.*, **44**, 152 (1976); *Catal. Rev. Sci. Eng.*, **14**, 153 (1976).
12) C. C. Kao, S. C. Tsai, M. K. Bahl, and Y. W. Chung, *Surf. Sci.*, **95**, 1 (1980).
13) Y. W. Chung and W. B. Weissbard, *Phys. Rev. B*, **20**, 3456 (1979); M. K. Bahl, S. C. Tsai, and Y. W. Chung, *Phys. Rev. B*, **21**, 1344 (1980).
14) J. A. Horsley, *J. Am. Chem. Soc.*, **101**, 2870 (1979).
15) K. H. Johnson, A. C. Balazs, and H. J. Kolari, *Surf. Sci*, **72**, 737 (1978).
16) B. Y. Lee, Y. Inoue, and I. Yasumori, unpublished.
17) G. H. Via, J. H. Sinfelt, and F. W. Lytle, *J. Chem. Phys.*, **71**, 690 (1979); R. B. Greegor, and F. W. Lytle, *J. Catal.*, **63**, 476 (1980).